PHYSICAL REVIEW A **100**, 043403 (2019)

Effective two-level models for highly efficient inner-state enantioseparation based on cyclic three-level systems of chiral molecules

Chong Ye,[1] Quansheng Zhang,[1] Yu-Yuan Chen,[1] and Yong Li[1,2,*]
[1]*Beijing Computational Science Research Center, Beijing 100193, China*
[2]*Synergetic Innovation Center for Quantum Effects and Applications, Hunan Normal University, Changsha 410081, China*

(Received 1 July 2019; published 10 October 2019)

Based on cyclic three-level systems of chiral molecules, we propose two methods to realize highly efficient inner-state enantioseparations of a chiral mixture with the two enantiomers initially prepared in their ground states. Our methods work in the region where the evolutions of the two enantiomers can be described by their corresponding effective two-level models, simultaneously. The approximately 100%-efficiency inner-state enantioseparations can be realized when the probability occupying the ground state of one enantiomer becomes zero by experiencing half-integer periods of its corresponding on-resonance Rabi oscillation and the other one stays always in the ground state approximately, under the conditions that the two enantiomers are governed by the effective on-resonance and large-detuning two-level models, respectively. Alternatively, the exactly 100%-efficiency inner-state enantioseparation can be obtained when the probability occupying the ground state of one enantiomer becomes zero by experiencing half-integer periods of its corresponding on-resonance Rabi oscillation and in the meanwhile that of the other one becomes 1 by experiencing integer periods of its corresponding detuned Rabi oscillation, respectively.

DOI: 10.1103/PhysRevA.100.043403

I. INTRODUCTION

Chirality is important in chemistry, biotechnologies, and pharmaceutics due to the fact that the vast majority of chemical [1], biological [2–4], and pharmaceutical [5–8] processes are chirality dependent. Yet, enantiodiscrimination [9] and enantioseparation [10–15] of a chiral mixture are among the most important and difficult tasks in chemistry. Some enantiodiscrimination [16–18] and enantioseparation methods [19,20] had been proposed based on the interferences between the electric and magnetic dipole transition moments. Since the magnetic dipole transition moments are usually very weak, alternative methods for enantiodiscrimination [21–29] and enantioseparation [30–38] based on only electric dipole transition moments had been proposed with the framework of three-level systems, where the transitions are driven in a cyclic manner [32–34,39–41]. For convenience, such systems are called cyclic three-level (or three-level Δ-type) systems.

The cyclic three-level systems of chiral molecules are special since the products of the corresponding three Rabi frequencies can change sign with enantiomers [21–38]. Accordingly, the two enantiomers will evolve differently with the same initial states. The inner-state enantioseparation of a chiral mixture is achieved if molecules in one of the three inner states are enantiopure (i.e., with only one enantiomer occupying that state). The probability of that state among the whole three states for that enantiomer can be defined as the efficiency of the inner-state enantioseparation. The enantiopure molecules in that state can be further spatially separated from the initial chiral mixture by a variety of energy-dependent processes [30,31]. In the original methods [30,31], the highly efficient inner-state enantioseparation was realized by means of the concepts from the adiabatic passage techniques [42], which make inner-state enantioseparation process [30,31] slow and complicated.

In order to overcome these defects in the adiabatic methods [30,31], a simple method has been introduced to promote the inner-state enantioseparation speed [36] by using shortcuts-to-adiabaticity techniques [43–45]. Comparing with the original adiabatical methods [30,31], the simpler and faster highly efficient inner-state enantioseparations can also be achieved by using only dynamic ultrashort-pulse operations [33,34]. Inspired by the recent breakthrough experiments in enantiodiscrimination [22–28] and enantioseparation [37,38], some works refocus on the related issues [46–52].

In this paper, we propose two dynamical methods to achieve highly efficient inner-state enantioseparation based on cyclic three-level systems. When the parameters are appropriately adjusted, the evolutions of the two enantiomers initially prepared in their corresponding ground states can be simultaneously described by effective two-level models with the same effective Rabi frequencies but different effective detunings. By further modifying the parameters to ensure that the effective two-level models for the two enantiomers are, respectively, on resonance and in the large-detuning limit, one can achieve the approximately 100%-efficiency inner-state enantioseparations when the probability occupying the ground state of the enantiomer governed by the effective on-resonance two-level model experiences half-integer periods of its Rabi oscillation. Alternatively, when one of the two-level models for the two enantiomers is on resonance and the other one is detuned (without requiring large detuning), one can

---

[*] liyong@csrc.ac.cn

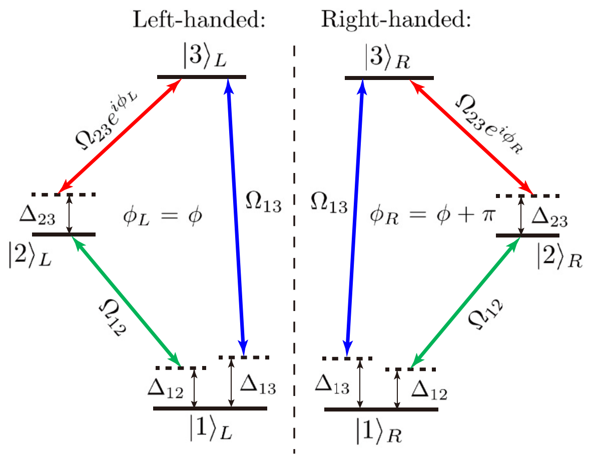

FIG. 1. Modeling the left- and right-handed enantiomers as cyclic three-level systems where three electromagnetic fields couple, respectively, to the three electric dipole transitions. For the left-handed enantiomer, the three corresponding Rabi frequencies are Ω_{12}, Ω_{13}, and $\Omega_{23}e^{i\phi}$. For the right-handed enantiomer, the three corresponding Rabi frequencies are Ω_{12}, Ω_{13}, and $\Omega_{23}e^{i(\phi+\pi)}$. The detunings for the three transitions are Δ_{12}, Δ_{13}, and Δ_{23}.

obtain exactly 100%-efficiency inner-state enantioseparations by making the probabilities occupying the ground states of the two enantiomers experience half-integer and integer periods of their corresponding Rabi oscillations, simultaneously. After achieving the inner-state enantioseparations by means of the above dynamical methods, the enantiopure molecules in the ground states can be further spatially separated by a variety of energy-dependent processes [30,31,36].

II. CYCLIC THREE-LEVEL SYSTEMS

The two enantiomers can be modeled simultaneously as cyclic three-level systems by choosing appropriate three electromagnetic fields to couple, respectively, with three electric dipole transitions [30–33] as shown in Fig. 1. Here, the inner states for the left- and right-handed enantiomers are $|j\rangle_L$ and $|j\rangle_R$ ($j = 1, 2, 3$), respectively. We assume they have the same energies $\hbar v_j$ by neglecting parity-violating energy differences due to the fundamental weak force. The scripts L and R have been introduced to denote the left-handed and right-handed enantiomers, respectively. The frequencies of the three electromagnetic fields are ω_{12}, ω_{13}, and ω_{23}, respectively. The detunings of the three transitions are defined as

$$\Delta_{ji} \equiv v_i - v_j - \omega_{ji}, \quad (3 \geqslant i > j \geqslant 1). \tag{1}$$

We are interested in the cases under the three-photon resonance with

$$\Delta_{12} + \Delta_{23} = \Delta_{13}, \tag{2}$$

i.e., $\omega_{12} + \omega_{23} = \omega_{13}$. In the rotating-wave approximation, the cyclic three-level systems for the two enantiomers can be described in the interaction picture as ($\hbar = 1$) [30,31]

$$\begin{aligned}\hat{H}_Q = {} & \Delta_{12}|2\rangle_{QQ}\langle 2| + \Delta_{13}|3\rangle_{QQ}\langle 3| + (\Omega_{12}|1\rangle_{QQ}\langle 2| \\ & + \Omega_{13}|1\rangle_{QQ}\langle 3| + \Omega_{23}e^{i\phi_Q}|2\rangle_{QQ}\langle 3| + \text{H.c.}),\end{aligned} \tag{3}$$

where $Q = L, R$ indicate the chirality. Without loss of generality, we assume Ω_{12}, Ω_{13}, and Ω_{23} are positive. Here ϕ_Q are the overall phases of the three Rabi frequencies for the two enantiomers. The chirality of the cyclic three-level systems is specified by choosing the overall phases of the left- and right-handed enantiomers as

$$\phi_L = \phi, \quad \phi_R = \phi + \pi \tag{4}$$

as shown in Fig. 1.

III. EFFECTIVE TWO-LEVEL MODELS

Initially, the two enantiomers are assumed to stay in their ground states $|1\rangle_{L,R}$ [30–36]. In the following, we will show that the evolution of the two enantiomers can be simultaneously described by their corresponding effective two-level models under the conditions

$$\Delta_{12} = \Delta_{13} \equiv \Delta, \quad \Omega_{12} = \Omega_{13} \equiv \Omega, \quad \phi = 0. \tag{5}$$

With the conditions (5), we can rewrite the Hamiltonian (3) for the two enantiomers as

$$\begin{aligned}\hat{H}_Q = {} & (\sqrt{2}\Omega|1\rangle_{QQ}\langle D_+| + \text{H.c.}) + \Delta_+^Q|D_+\rangle_{QQ}\langle D_+| \\ & + \Delta_-^Q|D_-\rangle_{QQ}\langle D_-|\end{aligned} \tag{6}$$

with

$$\Delta_\pm^L = \Delta \pm \Omega_{23}, \quad \Delta_\pm^R = \Delta \mp \Omega_{23}, \tag{7}$$

in the dressed state basis $\{|1\rangle_Q, |D_+\rangle_Q, |D_-\rangle_Q\}$ ($Q = L, R$) with

$$|D_\pm\rangle_Q = \frac{1}{\sqrt{2}}(|2\rangle_Q \pm |3\rangle_Q). \tag{8}$$

Since $|D_-\rangle_Q$ decouples with the other states $|1\rangle_Q$ and $|D_+\rangle_Q$, the two enantiomers, initially prepared in their ground states $|1\rangle_Q$, will not evolve to the dressed state $|D_-\rangle_Q$, and can be described by the effective two-level models with

$$\hat{H}_Q^{\text{eff}} = (\sqrt{2}\Omega|1\rangle_{QQ}\langle D_+| + \text{H.c.}) + \Delta_+^Q|D_+\rangle_{QQ}\langle D_+|. \tag{9}$$

For the two enantiomers, their corresponding effective Rabi frequencies are $\sqrt{2}\Omega$. The effective two-level models are chirality dependent since the effective detunings are different $\Delta_+^L \neq \Delta_+^R$. In Fig. 2, we show the cyclic three-level models for the two enantiomers can reduce to the effective two-level ones under the condition (5).

We would like to note that when $\phi = 0$ changes to be $\phi = \pi$ in the condition (5), one will obtain the similar results of effective two-level models except the forms of the Hamiltonian for the two enantiomers exchanging with each other. For convenience, we will focus on the cases with $\phi = 0$.

IV. HIGHLY EFFICIENT INNER-STATE ENANTIOSEPARATIONS

So far we have shown that the cyclic three-level systems for the enantiomers can reduce to the chirality-dependent effective two-level models. Further, we will propose two methods to realize highly efficient inner-state enantioseparation with the zero and (approximate) 1 probabilities of the ground state

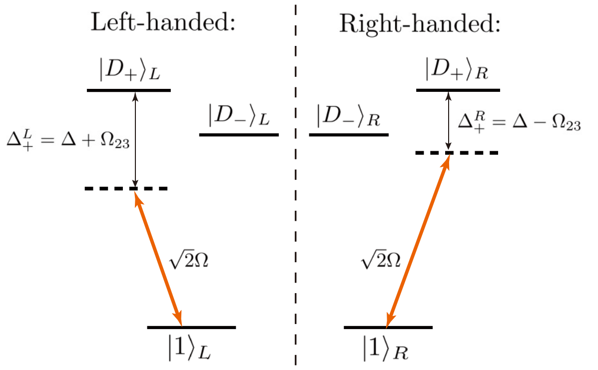

FIG. 2. Chirality-dependent effective two-level models for the two enantiomers initial prepared in their ground states under the condition (5): $\Delta_{12} = \Delta_{13} \equiv \Delta$, $\Omega_{12} = \Omega_{12} \equiv \Omega$, $\phi = 0$, and $\Delta_{23} = 0$. The dressed states are $|D_+\rangle_Q = (|2\rangle_Q + |3\rangle_Q)/\sqrt{2}$ and $|D_-\rangle_Q = (|2\rangle_Q - |3\rangle_Q)/\sqrt{2}$. The effective Rabi frequency is $\sqrt{2}\Omega$ and the effective detunings are $\Delta_+^L = \Delta + \Omega_{23}$ and $\Delta_+^R = \Delta - \Omega_{23}$.

for the two enantiomers, respectively. After that, the two enantiomers in different energy states can be spatially separated by a variety of energy-dependent processes [30,31,36].

For the two enantiomers of initial ground states, their evolved states are governed by Eq. (9) with the corresponding probabilities occupying the ground states

$$P_1^Q(t) = \frac{4\Omega^2}{\omega_Q^2}[\cos(\omega_Q t) - 1] + 1, \quad (Q = L, R) \tag{10}$$

where the Rabi oscillation frequencies of the probabilities occupying the ground states are

$$\omega_{L,R} = \sqrt{8\Omega^2 + (\Delta \pm \Omega_{23})^2}. \tag{11}$$

Here the index L on the left-hand side corresponds to the positive sign on the right-hand side.

Here we just focus on the condition

$$\Omega_{23} = \Delta. \tag{12}$$

Then, the Rabi oscillation frequencies of the probabilities occupying the ground states are $\omega_L = 2\sqrt{2\Omega^2 + \Delta^2}$ and $\omega_R = 2\sqrt{2}\Omega$, and the corresponding Rabi oscillation periods are

$$T_L = \frac{\pi}{\sqrt{2\Omega^2 + \Delta^2}}, \quad T_R = \frac{\sqrt{2}\pi}{2\Omega}. \tag{13}$$

In what follows, we will show two methods of inner-state enantiomer separation under the condition (12) as well as the condition (5), by generating the different probabilities occupying the ground states for the two enantiomers.

A. Approximately 100%-efficiency inner-state enantioseparations

Here we propose the first method to realize the approximately 100%-efficiency inner-state enantioseparations with $P_1^R = 0$ and $P_1^L \simeq 1$ based on the conditions (5) and (12) and the following one:

$$\Delta \gg \Omega. \tag{14}$$

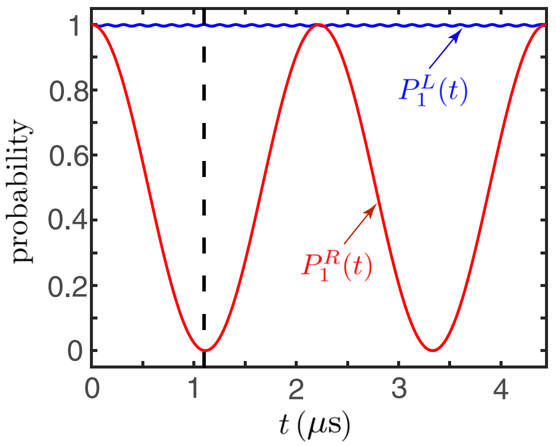

FIG. 3. Approximately 100%-efficiency inner-state enantioseparations. The probabilities occupying the ground states of the left-handed enantiomer $P_1^L(t)$ are denoted by the blue line, and those of the right-handed enantiomer $P_1^R(t)$ are denoted by the red line. The parameters are $\phi = 0$, $\Delta_{12} = \Delta_{13} \equiv \Delta = 20\,\mathrm{MHz}$, $\Omega_{23} = 20\,\mathrm{MHz}$, and $\Omega_{12} = \Omega_{13} \equiv \Omega = 1\,\mathrm{MHz}$. According to the three-photon resonance condition, we have $\Delta_{23} = 0\,\mathrm{MHz}$. The approximately 100%-efficiency inner-state enantioseparation is achieved at, e.g., $t = \sqrt{2}\pi/4\,\mu\mathrm{s}$ (black dashed line) with $P_1^L = 0.9998 \simeq 1$ and $P_1^R = 0$.

In this case, the effective two-level models of the two enantiomers are, respectively, in the large-detuning limit and on resonance:

$$\Delta_+^L = 2\Delta \gg \sqrt{2}\Omega, \quad \Delta_+^R = 0. \tag{15}$$

For the left-handed enantiomer, it will always stay approximately in the initial state $|1\rangle_L$ due to the large-detuning coupling. On the other hand, the right-handed enantiomer can be totally transferred to the state $|D_+\rangle_R$ at the time instant

$$t = \left(n + \tfrac{1}{2}\right)T_R \tag{16}$$

with the integer $n \geqslant 0$, i.e., when the probability occupying the ground state of the right-handed enantiomer experiences half-integer periods of its Rabi oscillation. The corresponding probability occupying the ground state for the left-handed enantiomer is $P_1^L(t)$, which satisfies $1 \geqslant P_1^L(t) \geqslant (1 - 4\Omega^2/\sqrt{2\Omega^2 + \Delta^2}) \simeq 1$. Thus the approximately 100%-efficiency inner-state enantioseparations are achieved.

In Fig. 3, by evaluating Eq. (10), we demonstrate the approximately 100%-efficiency inner-state enantioseparations by referring to the typical experimental parameters [37,38] $\Delta_{12} = \Delta_{13} \equiv \Delta = \Omega_{23} = 20\,\mathrm{MHz}$ and $\Omega_{12} = \Omega_{13} = \Omega = 1\,\mathrm{MHz}$. We assume the two enantiomers are initially prepared in their ground states [30–36]. As expected, the left-handed enantiomer still stays approximately in the ground state during the evolution. The probability occupying the ground state of the right-handed enantiomer experiences a half period of its Rabi oscillation and then becomes $P_1^R = 0$. In the meanwhile, $P_1^L = 0.9998 \simeq 1$ (see the dashed line in Fig. 3). This clearly indicates a highly efficient inner-state enantioseparation with efficiency of 99.98%. This efficiency can be further improved by increasing Δ and/or decreasing Ω. Similarly, we can also realize the approximately 100%-efficiency inner-state enantioseparations with $P_1^L = 0$ and $P_1^R \simeq 1$ since

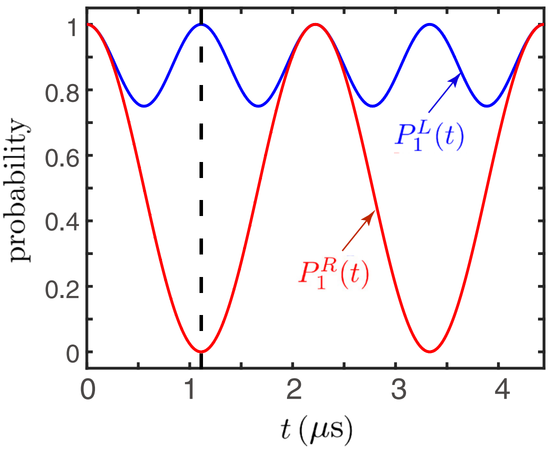

FIG. 4. Exactly 100%-efficiency inner-state enantioseparations. The probabilities occupying the ground states of the left-handed enantiomer $P_1^L(t)$ are denoted by the blue line, and those of the right-handed enantiomer $P_1^R(t)$ are denoted by the red line. The parameters are $\phi = 0$, $\Delta_{12} = \Delta_{13} \equiv \Delta = \sqrt{6}$ MHz, $\Omega_{23} = \sqrt{6}$ MHz, $\Omega_{12} = \Omega_{13} \equiv \Omega = 1$ MHz, and $\Delta_{23} = 0$ MHz. The exactly 100%-efficiency inner-state enantioseparations are achieved at $t = \sqrt{2}\pi/4\ \mu$s (black dashed line) with $P_1^L = 1$ and $P_1^R = 0$, when the probabilities of the two enantiomers experience integer (1) and half-integer (1/2) periods of their corresponding Rabi oscillations.

the evolved probabilities of the two enantiomers occupying the ground state exchange with each other by changing Δ to its opposite value [seen from Eq. (10)] or replacing $\phi = 0$ in Eq. (5) by $\phi = \pi$.

B. Exactly 100%-efficiency inner-state enantioseparations

In our first method, the large detuning is needed and the efficiency of inner-state enantiomer separation is approximately 100%. Alternatively, we will propose a method without the requirement of the large detuning to achieve 100%-efficiency enantiomer separation. This would happen if

$$P_1^L(t) = 1, \quad P_1^R(t) = 0. \tag{17}$$

This will happen when the probabilities occupying the ground states of the left- and right-handed enantiomers experience integer and half-integer periods of their corresponding Rabi oscillations, simultaneously. That means it happens at the time instant satisfying

$$t = n_L T_L = \left(n_R + \tfrac{1}{2}\right) T_R, \quad (n_L > n_R \geqslant 0), \tag{18}$$

which requires

$$\Delta = \frac{\sqrt{8n_L^2 - 2(2n_R + 1)^2}}{2n_R + 1}\Omega, \quad (n_L > n_R \geqslant 0). \tag{19}$$

In Fig. 4, by evaluating Eq. (10), we demonstrate the exactly 100%-efficiency inner-state enantioseparations for the typical experimental parameters [37,38] with $\Delta_{12} = \Delta_{13} \equiv \Delta = \sqrt{6}$ MHz, $\Omega_{23} = \sqrt{6}$ MHz, $\Omega_{12} = \Omega_{13} \equiv \Omega = 1$ MHz under the conditions (5), (12), and (19) with $n_L = 1$ and $n_R = 0$. It clearly shows exactly 100%-efficiency inner-state separation with $P_1^L = 1$ and $P_1^R = 0$ simultaneously. Similarly, we can also realize the exactly 100%-efficiency inner-state enantioseparations with $P_1^L = 0$ and $P_1^R = 1$ since the evolutions of the two enantiomers exchange with each other by changing Δ to its opposite value or choosing $\phi = \pi$.

V. SUMMARY

We have proposed two methods to achieve highly efficient inner-state enantioseparations based on the cyclic three-level systems of chiral molecules. Then, the enantiopure molecules in the ground state can be further spatially separated by the energy-dependent processes [30,31,36]. By choosing the appropriate parameters under the three-photon resonance condition, the two enantiomers initially prepared in their corresponding ground states $|1\rangle_Q$ can be governed by chirality-dependent effective two-level models in the basis $\{|1\rangle_Q, |D_+\rangle_Q\}$ with $Q = L, R$. Their corresponding effective two-level models have the same effective Rabi frequencies but different effective detunings. The approximately 100%-efficiency inner-state enantioseparations can be realized when the effective two-level model for one enantiomer is on resonance and that for the other enantiomer is largely detuned. Specifically, the probability occupying the ground state of the enantiomer becomes zero with the half integer of its on-resonance Rabi oscillation and in the meanwhile the other enantiomer stays approximately in the ground state. Moreover, we have proposed the second method to realize exactly 100%-efficiency inner-state enantioseparations, when the probabilities occupying the ground states of the two enantiomers experience half-integer and integer periods of their corresponding on-resonance and detuned Rabi oscillations, simultaneously.

Comparing with the original adiabatical inner-state enantioseparation methods based on three-level systems of chiral molecules [30,31], our two methods are faster and simpler since they are based on the dynamical evolutions of the two enantiomers governed by the simple chirality-dependent effective two-level models. Actually, our methods are similar to the dynamical inner-state enantioseparation methods based on three-level systems [33,34] with reducing the three-level models of the two enantiomers to effective two-level ones. However, our methods require less steps than the dynamic methods [33,34] to realize the inner-state enantioseparation. Comparing with the shortcuts-to-adiabaticity method for enantioseparation based on three-level systems [36] where the parameters are time-dependently controlled to fulfill the condition of shortcuts to adiabaticity, our methods are simpler since the parameters are time independent in our proposals.

We would like to remark that the overall phase ϕ (or $\phi + \pi$) is crucial in the experimental scheme. In practice, the phase ϕ can be chosen by appropriately adjusting the initial phases of the three electromagnetic fields. When the characteristic length of the apparatus is much smaller than the typical wavelengths of the three electromagnetic fields, the phase ϕ can be maintained throughout the entire sample and is the same for all molecules. Note that our two methods work only for C_1-symmetric chiral molecules when the rotational transitions of gaseous molecules are considered. Correspondingly, the polarizations of the three electromagnetic fields should be mutual vertical to each other and the rotational parts of the three states should be well chosen to construct the cyclic three-level systems [49,50]. For C_n- or D_n-symmetric gaseous chiral molecules (with $n > 1$), our two methods fail since at least two of the electric dipole moment projections vanish. We also note that the temperature effect is one of the major obstacles in realistic experiments. In our future work, we will further investigate how to suppress such an effect of temperature in inner-state enantioseparation.

ACKNOWLEDGMENTS

This work was supported by National Key Research and Development Program of China Grant No. 2016YFA0301200; National Natural Science Foundation of China Grants No. 11774024, No. 11534002, No. U1930402, and No. U1730449; and Science Challenge Project Grant No. TZ2018003.

[1] H. P. Latscha, U. Kazmaier, and H. A. Klein, *Organische Chemie*, 6th ed. (Springer-Verlag, Berlin, 2008).
[2] J. Gal, Chirality **12**, 959 (2012).
[3] T. J. Leitereg, D. G. Guadagni, J. Harris, T. R. Mon, and R. Teranishi, J. Agric. Food Chem. **19**, 785 (1971).
[4] J. Hyttel, K. Bøgesø, J. Perrgaard, and C. Sánchez, J. Neural Transm. **88**, 157 (1992).
[5] A. J. Hutt and S. C. Tan, Drugs **52**, 1 (1996).
[6] E. J. Ariens, Eur. J. Clin. Pharmacol. **26**, 663 (1984).
[7] T. Eriksson, S. Bjorkman, and P. Hoglund, Eur. J. Clin. Pharmacol. **57**, 365 (2001).
[8] S. K. Teo, W. A. Colburn, W. G. Tracewell, K. A. KookDavid, I. Stirling, M. S. Jaworsky, M. A. Scheffler, S. D. Thomas, and O. L. Laskin, Clin. Pharmacokinet. **43**, 311 (2004).
[9] W. S. Knowles, Angew. Chem., Int. Ed. Engl. **41**, 1998 (2002) (Nobel lecture 2001).
[10] K. Bodenhöfer, A. Hierlemann, J. Seemann, G. Gauglitz, B. Koppenhoefer, and W. Gpel, Nature (London) **387**, 577 (1997).
[11] R. McKendry, M.-E. Theoclitou, T. Rayment, and C. Abell, Nature (London) **391**, 566 (1998).
[12] G. L. J. A. Rikken and E. Raupach, Nature (London) **405**, 932 (2000).
[13] H. Zepik, E. Shavit, M. Tang, T. R. Jensen, K. Kjaer, G. Bolbach, L. Leiserowitz, I. Weissbuch, and M. Lahav, Science **295**, 1266 (2002).
[14] R. Bielski and M. Tencer, J. Sep. Sci. **28**, 2325 (2005); Origins Life Evol. Biosphere **37**, 167 (2007).
[15] *Chiral Analysis*, edited by K. W. Busch and M. A. Busch (Elsevier, Amsterdam, 2006).
[16] Y. He, B. Wang, R. K. Dukor, and L. A. Nafie, Appl. Spectrosc. **65**, 699 (2011).
[17] P. J. Stephens, J. Phys. Chem. **89**, 748 (1985).
[18] M. M. R. Fanood, N. B. Ram, C. S. Lehmann, I. Powis, and M. H. M. Janssen, Nat. Commun. **6**, 7511 (2015).
[19] C. Brand, B. A. Stickler, C. Knobloch, A. Shayeghi, K. Hornberger, and M. Arndt, Phys. Rev. Lett. **121**, 173002 (2018).
[20] F. Suzuki, T. Momose, and S. Y. Buhmann, Phys. Rev. A **99**, 012513 (2019).
[21] E. Hirota, Proc. Jpn. Acad. Ser. B **88**, 120 (2012).
[22] D. Patterson, M. Schnell, and J. M. Doyle, Nature (London) **497**, 475 (2013).
[23] D. Patterson and J. M. Doyle, Phys. Rev. Lett. **111**, 023008 (2013).
[24] D. Patterson and M. Schnell, Phys. Chem. Chem. Phys. **16**, 11114 (2014).
[25] V. A. Shubert, D. Schmitz, D. Patterson, J. M. Doyle, and M. Schnell, Angew. Chem., Int. Ed. **53**, 1152 (2014).
[26] V. A. Shubert, D. Schmitz, C. Medcraft, A. Krin, D. Patterson, J. M. Doyle, and M. Schnell, J. Chem. Phys. **142**, 214201 (2015).
[27] S. Lobsiger, C. Perez, L. Evangelisti, K. K. Lehmann, and B. H. Pate, J. Phys. Chem. Lett. **6**, 196 (2015).
[28] V. A. Shubert, D. Schmitz, C. Pérez, C. Medcraft, A. Krin, S. R. Domingos, D. Patterson, and M. Schnell, J. Phys. Chem. Lett. **7**, 341 (2015).
[29] K. K. Lehmann, *Theory of Enantiomer-Specific Microwave Spectroscopy* (Elsevier, Amsterdam, 2017).
[30] P. Král and M. Shapiro, Phys. Rev. Lett. **87**, 183002 (2001).
[31] P. Král, I. Thanopulos, M. Shapiro, and D. Cohen, Phys. Rev. Lett. **90**, 033001 (2003).
[32] Y. Li, C. Bruder, and C. P. Sun, Phys. Rev. Lett. **99**, 130403 (2007).
[33] Y. Li and C. Bruder, Phys. Rev. A **77**, 015403 (2008).
[34] W. Z. Jia and L. F. Wei, J. Phys. B **43**, 185402 (2010).
[35] X. Li and M. Shapiro, J. Chem. Phys. **132**, 194315 (2010).
[36] N. V. Vitanov and M. Drewsen, Phys. Rev. Lett. **122**, 173202 (2019).
[37] S. Eibenberger, J. Doyle, and D. Patterson, Phys. Rev. Lett. **118**, 123002 (2017).
[38] C. Perez, A. L. Steber, S. R. Domingos, A. Krin, D. Schmitz, and M. Schnell, Angew. Chem., Int. Ed. **56**, 12512 (2017).
[39] N. A. Ansari, J. Gea-Banacloche, and M. S. Zubairy, Phys. Rev. A **41**, 5179 (1990).
[40] Y.-X. Liu, J. Q. You, L. F. Wei, C. P. Sun, and F. Nori, Phys. Rev. Lett. **95**, 087001 (2005).
[41] L. Zhou, L.-P. Yang, Y. Li, and C. P. Sun, Phys. Rev. Lett. **111**, 103604 (2013).
[42] N. V. Vitanov, A. A. Rangelov, B. W. Shore, and K. Bergmann, Rev. Mod. Phys. **89**, 015006 (2017).
[43] R. G. Unanyan, L. P. Yatsenko, K. Bergmann, and B. W. Shore, Opt. Commun. **139**, 48 (1997).
[44] M. Demirplak and S. A. Rice, J. Phys. Chem. A **107**, 9937 (2003).
[45] X. Chen, I. Lizuain, A. Ruschhaupt, D. Guéry-Odelin, and J. G. Muga, Phys. Rev. Lett. **105**, 123003 (2010).
[46] K. K. Lehmann, J. Chem. Phys. **149**, 094201 (2018).
[47] T. Kh. Begzjav, Zhedong Zhang, M. O. Scully, and G. S. Agarwal, Opt. Express **27**, 13965 (2019).
[48] A. A. Milner, J. A. M. Fordyce, I. MacPhail-Bartley, W. Wasserman, V. Milner, I. Tutunnikov, and I. Sh. Averbukh, Phys. Rev. Lett. **122**, 223201 (2019).
[49] C. Ye, Q. Zhang, and Y. Li, Phys. Rev. A **98**, 063401 (2018).
[50] C. Ye, Q. Zhang, and Y. Li, Phys. Rev. A **99**, 062703 (2019).
[51] M. Leibscher, T. F. Giesen, and C. P. Koch, J. Chem. Phys. **151**, 014302 (2019).
[52] C. Ye, Q. Zhang, Y.-Y. Chen, and Y. Li, Phys. Rev. A **100**, 033411 (2019).